Supporting Information

Isolation and Characterization of a Blue Coloured Three Coordinate Cu(I)-radical Complex with a S_3 Donor Set

Sujit Das,[a] Sonam Suthar,[a] Maria Francis,[b] Saurav Ghosh,[a] Sangita Mondal,[a] Sunil Kumar,[a] and Kartik Chandra Mondal*[a]

[a] Department of Chemistry, Indian Institute of Technology Madras, Chennai 600036, India. **E-mail:** csdkartik@iitm.ac.in

[b] Department of Chemistry, IISER Tirupati, AP, India

General Synthesis:

All the organic solvents (THF, *n*-hexane, toluene, C_6D_6) were soaked with 3 Å molecular sieves to removed water and followed by distillation with Na metal and NaK alloy three times under the flow of high purity argon gas. All the manipulations were performed inside the glove box running with argon gas below H_2O/O_2 level of 10 ppm. The mixture of dithiolene radical anion [(THF)$_2$Li(SS-NHC=S)]/S-NHCH was prepared by following the previously reported synthetic method.[S1] X-ray single crystal mounted was performed using paratone oil under flow of argon gas and data were collected in Bruker D8 VENTURE model (machine) at 100 K and 150 K. Data was refined using Apex-4 package. CV was measured in alloy distilled THF in potentiometer (Mterohm). NMR was recorded in C_6D_6 in 500 MHz Bruker instrument at IIT Madras. EPR was simulated using EASY-SPIN package.

Synthesis of complex [Cu^I(S-NHCH)(SS-NHC=S)] (**1**)**:** A reported mixture of ligands [(THF)$_2$Li(SS-NHC=S)] (radical anion) and $^-$S-NHCH$^+$ (C4 thiolated and C2-protonated zwitterionic NHC carbene) was synthesis synthesized following the reported literature procedure by reacting free NHC with BuLi and followed by stepwise reaction with sulfur powder in THF/ether solution.[1] The mixture of dithiolene radical anion [(THF)$_2$Li(SS-NHC=S)]/ $^-$S-NHCH$^+$ (253 mg; 0.4 mmol; calculated based on the MW of the radical anion) was place in a 100 mL Schlenk flask and dissolved in THF (15 mL), resulting in a dark purple solution after 10 min of stirring at room temperature (rt). Concurrently, anhydrous CuCl (19.8 mg, 0.2 mmol) was separately dissolved in 8 mL of THF in another Schlenk flask. The resultant solutions were mixed via a cannula causing a colour change from dark purple to intense violet,

indicating the onset of a chemical reaction. The reaction mixture was stirred for 4-5 h to ensure complete conversion. The THF solvent was then removed under vacuum, yielding a dry mass. This mass was further treated with a mixture of *n*-hexane and THF (3:1 ratio, total volume 15 mL) to obtain a violate coloured solution. After storing the resultant solution at room temperature for one day the colour of the solution changed to greenish violet from which dark blue needles of complex **1** were formed. The crystals were separated from the mother liquor using a syringe inside the glove box and flashed washed with *n*-hexane and subsequently dried under vacuum. Isolated amount 77 mg. The yield is 40% (based on Cu). IR (KBr, cm^{-1}): 2972, 2859, 1641, 1258, 1099, 1035, 807, 692. UV-vis band at 420, 554, 658 nm. C, H, N analysis % (calcd): C 67.43 (67.15), H 7.05 (7.20), N 5.72 (5.80). Pure single crystals were isolated (after removal of mother liquor using a syringe; washed with could *n*-hexane) which were grinded to form powers required for all other characterizations (EPR, UV-sis, NMR and CV).
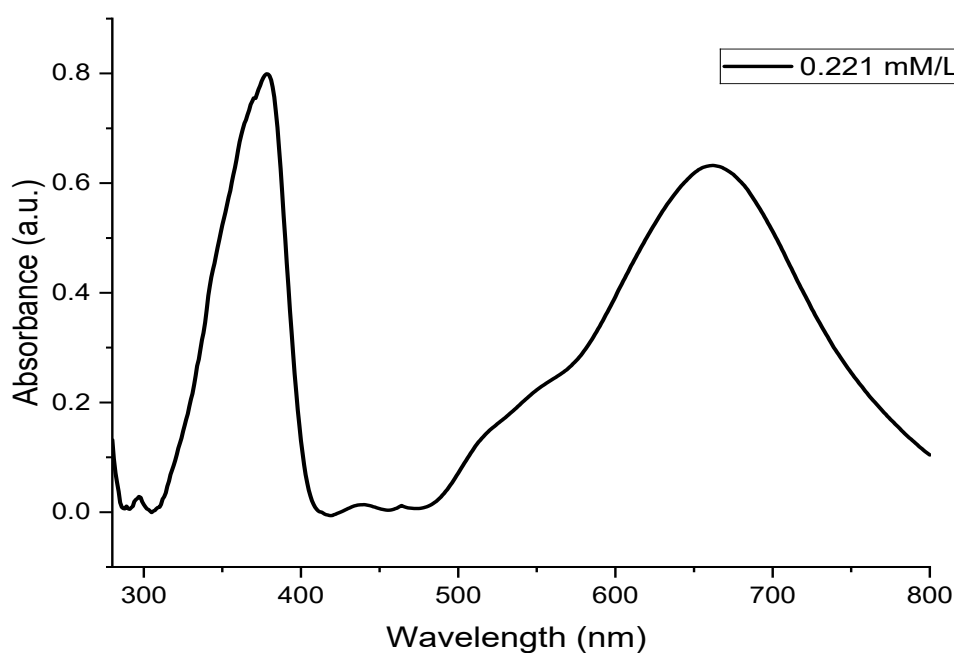

Figure S1. UV-Vis absorption spectrum of THF solution (2.21×10^{-4} M/L) of complex [Cu^{I}(S-NHCH)(SS-NHC=S)] (**1**).

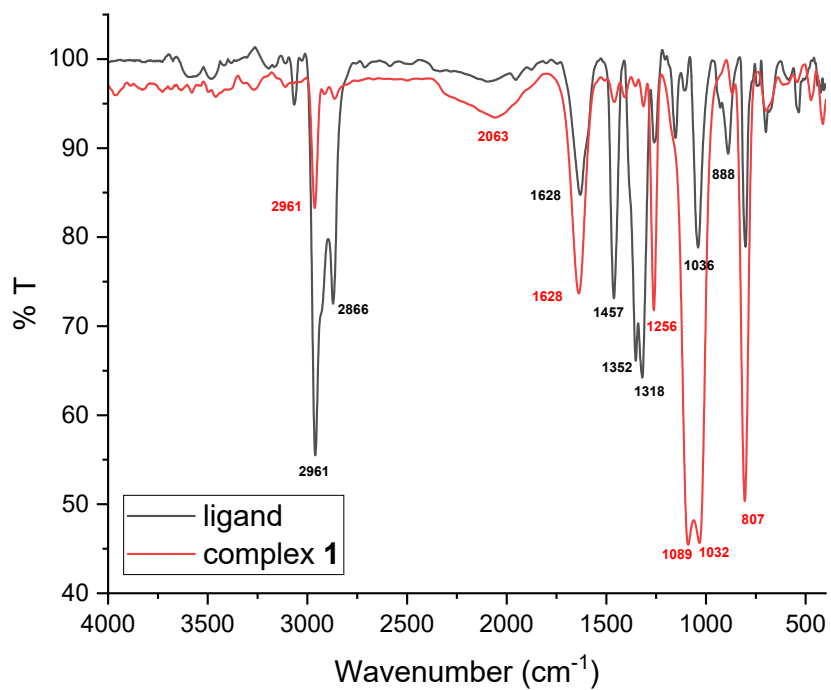**Figure S2.** FT-IR spectrum of $[Cu^I(S\text{-}NHCH)(SS\text{-}NHC=S)]$ (**1**) with dry KBr. Sample was prepared inside the glove box at rt. KBr has been dried by heating at 250 °C under vacuum prior to sample preparation.
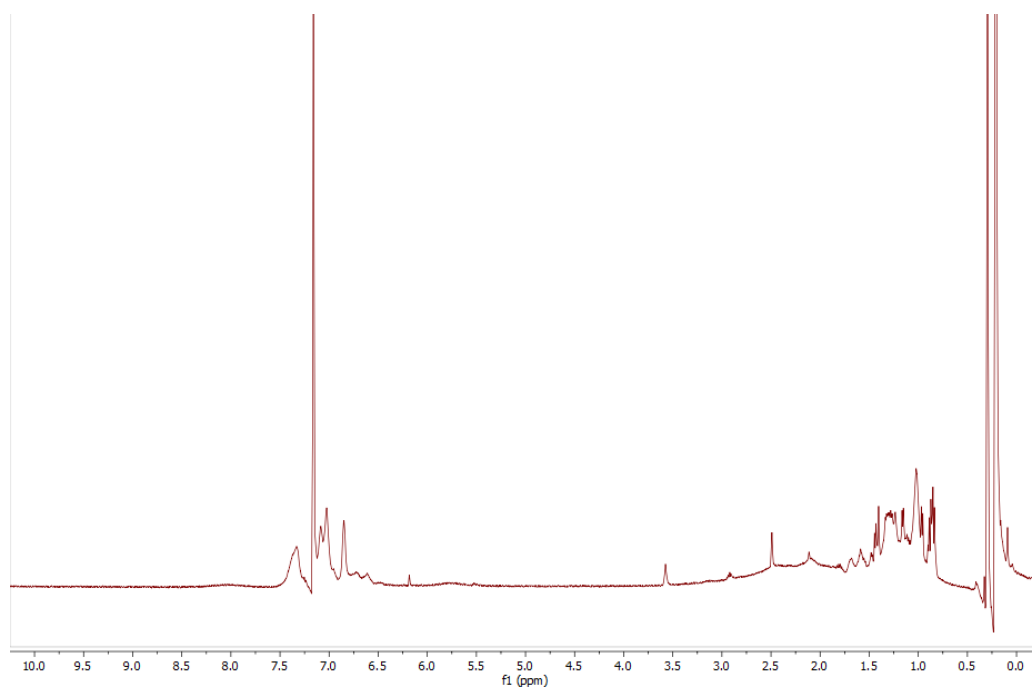

Figure S3. ^{1}H NMR spectrum of complex $[Cu^I(S\text{-}NHCH)(SS\text{-}NHC=S)]$ (**1**) in C_6D_6 at room temperature (500 MHz).

Table S1. Crystallographic details of [Cu^I(S-NHCH)(SS-NHC=S)] (**1**):

CCDC Deposit	2349133
Empirical formula	$C_{108}H_{139}Cu_2N_8S_8$
Formula weight	1932.82
Temperature (K)	100 (2)
Wavelength (Å)	0.71073
Crystal system	Monoclinic
Space group	$P\,2_1/c$
Unit cell dimensions	a = 15.3152 (8) Å b = 40.9418 (19) Å c = 20.7779 (10) Å α = 90° β = 98.274 (2)° γ = 90°
Volume (Å^3)	12892.8 (11)
Z	4
Density (Mg/m^3)	0.996
Absorption coefficient (mm^{-1})	0.500
F (000)	4116
Crystal size (mm^3)	0.400 x 0.388 x 0.150
Theta range for data collection (°)	1.791 to 25.098
Index ranges	-18<=h<=18 -48<=k<=48 -24<=l<=23
R (int)	0.1214
Reflections collected	347138
Independent reflections	22826
Completeness to theta = 25.242°	99.5 %
Max. and min. transmission	0.7454 and 0.5849
Number of Restraints	1311
Number of Parameters	1465
Refinement method	Full-matrix least-squares on F^2
Final R indices [I>2sigma(I)]	R_1 = 0.0552, wR_2 = 0.1767
R indices (all data)	R_1 = 0.1065, wR_2 = 0.2350
$GooF$	0.829
Largest diff. peak and hole [e·Å^{-3}]	0.535 and -0.717
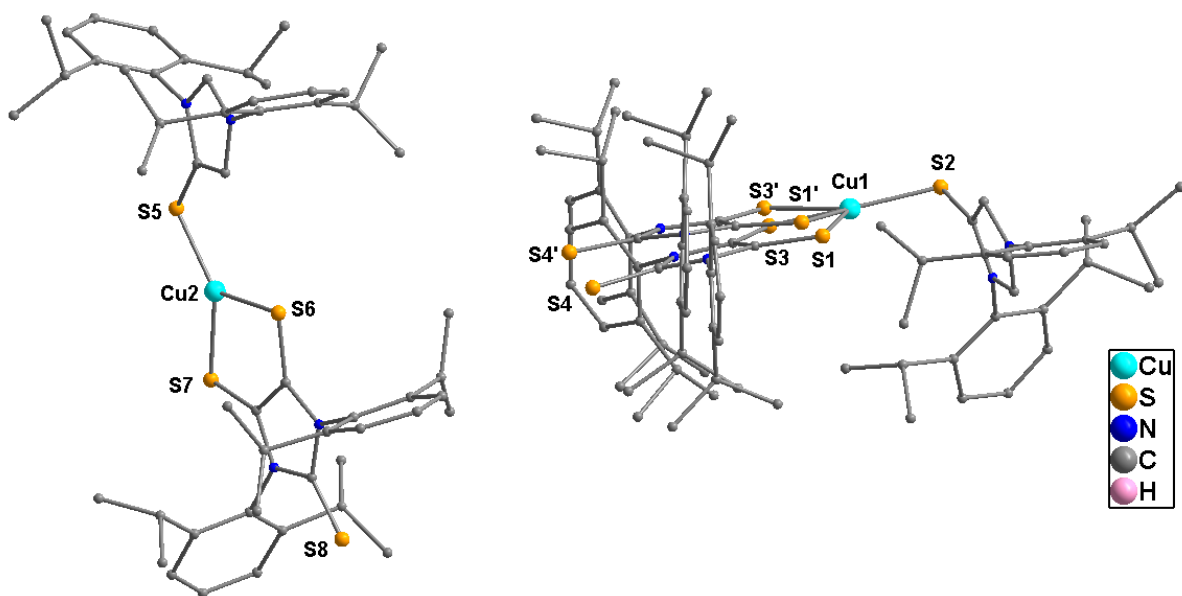
Figure S4. The structures of two independent molecules of complex [Cu^I(S-NHCH)(SS-NHC=S)] (**1**) in the crystallographic asymmetric unit. H-atoms were omitted for clarity. Selected bond lengths and bond angles were given in Tables S2-S3. The dithiolene radical unit of the molecule at the right side is disordered. Data collected at 100 K.

Table S2. Selected bond lengths [Å] for the complex [Cu^I(S-NHCH)(SS-NHC=S)] (**1**).

Cu(1)-S(3)	2.134(7)	S(3')-C(8')	1.704(14)
Cu(1)-S(2)	2.1806(10)	S(1')-C(7')	1.672(16)
Cu(1)-S(1')	2.260(4)	S(4)-C(9)	1.667(10)
Cu(1)-S(3')	2.407(8)	S(6)-C(88)	1.684(4)
Cu(1)-S(1)	2.407(7)	S(5)-C(65)	1.731(3)
Cu(2)-S(5)	2.1528(10)	S(7)-C(94)	1.677(4)
Cu(2)-S(7)	2.2530(11)	C(8)-S(3)	1.657(18)
Cu(2)-S(6)	2.2928(11)	C(7)-S(1)	1.660(17)
S(8)-C(45)	1.647(4)	C(9')-S(4')	1.660(9)
S(2)-C(14)	1.738(4)		

Table S3. Selected bond angles [°] for the complex [Cu^I(S-NHCH)(SS-NHC=S)] (**1**).

S(3)-Cu(1)-S(2)	142.5(3)	S(2)-Cu(1)-S(3')	132.9(2)
S(2)-Cu(1)-S(1')	131.5(3)	S(1')-Cu(1)-S(3')	94.7(2)

S(3)-Cu(1)-S(1)	98.10(14)	C(7')-S(1')-Cu(1)	96.9(6)
S(2)-Cu(1)-S(1)	118.8(3)	C(88)-S(6)-Cu(2)	93.64(14)
S(5)-Cu(2)-S(7)	133.46(4)	C(65)-S(5)-Cu(2)	104.40(11)
S(5)-Cu(2)-S(6)	128.33(4)	C(94)-S(7)-Cu(2)	94.48(14)
S(7)-Cu(2)-S(6)	98.17(4)	C(8)-S(3)-Cu(1)	96.5(7)
C(14)-S(2)-Cu(1)	99.09(12)	C(7)-S(1)-Cu(1)	90.6(6)
C(8')-S(3')-Cu(1)	93.2(5)		

…………………………………………………………………………………………………..
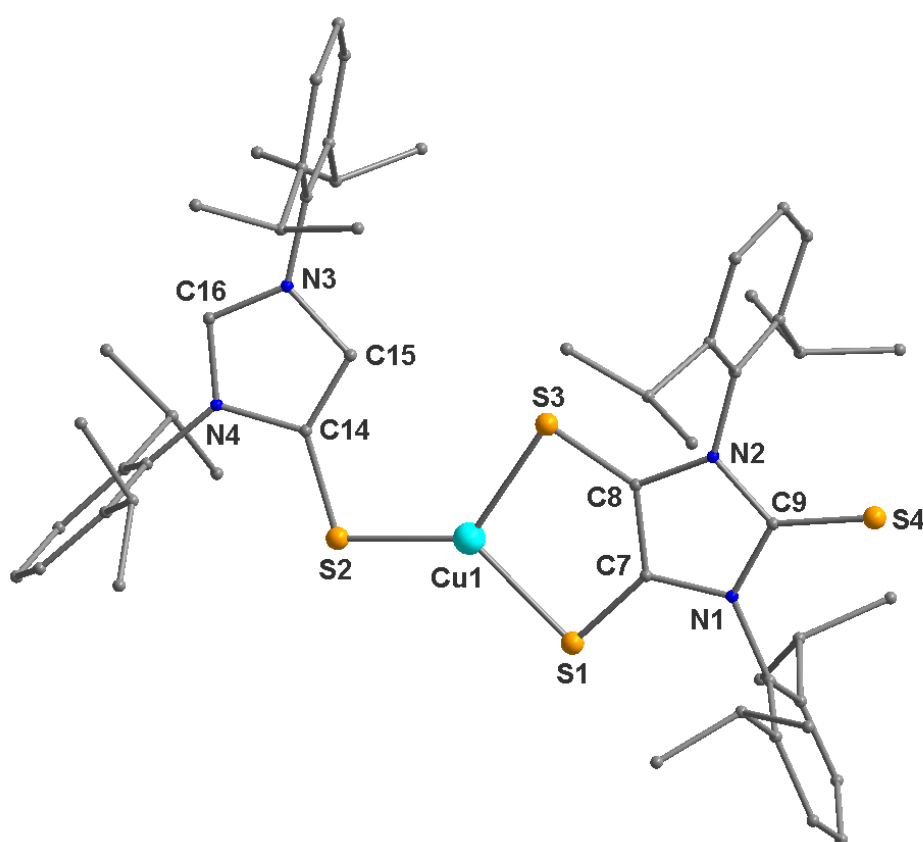
Figure S5. Molecular structure of complex [Cu^I(S-NHCH)(SS-NHC=S)] (**1**). H-atoms were omitted for clarity. Selected bond lengths (Å) and angles (°): C14-S2 1.740(5), C7-S1 1.692(16), C8-S3 1.655(14), C7-C8 1.405(19), C9-S4 1.630(17), Cu1-S1 2.240(9), Cu1-S2 2.1508(15), Cu1-S3 2.321(7); S1-Cu1-S2 133.1(2), S2-Cu1-S3 127.26(17), S1-Cu1-S3 97.5(3). Values are reported for one of the molecules of **1**. Data collected at 150 K. There were two molecules of **1** in the crystallographic asymmetric unit. The molecular structure of the less disordered molecular unit has been represented here.

Table S4. Crystallographic details of the complex [Cu^I(S-NHCH)(SS-NHC=S)] (**1**). Data collected at 150 K.

Empirical formula	C$_{108}$H$_{139}$Cu$_2$N$_8$S$_8$
Formula weight	1932.82
Temperature (K)	150 (2)
Wavelength (Å)	0.71073
Crystal system	Monoclinic
Space group	$P\,2_1/c$
Unit cell dimensions	a = 15.4824 (13) Å
	b = 41.126 (3) Å
	c = 20.8766 (16) Å
	α = 90°
	β = 98.405 (4)°
	γ = 90°
Volume (Å^3)	13149.9 (18)
Z	4
Density (Mg/m^3)	0.976
Absorption coefficient (mm^{-1})	0.490
F (000)	4112
Crystal size (mm^3)	0.138 x 0.013 x 0.011
Theta range for data collection (°)	1.827 to 26.543
Index ranges	-19<=h<=19
	-51<=k<=51
	-26<=l<=26
R (int)	0.4019
Reflections collected	799953
Independent reflections	27191
Completeness to theta = 25.242°	100.0 %
Max. and min. transmission	0.7454 and 0.5849
Number of Restraints	2406
Number of Parameters	1723
Refinement method	Full-matrix least-squares on F^2
Final R indices [I>2sigma(I)]	R_1 = 0.0787, wR_2 = 0.1861
R indices (all data)	R_1 = 0.2004, wR_2 = 0.592
$GooF$	1.005
Largest diff. peak and hole [e·Å^{-3}]	0.494 and -0.592

Table S5. Selected bond lengths [Å] for the complex [Cu^I(S-NHCH)(SS-NHC=S)] (**1**).

Cu(1)-S(2)	2.1508(15)	S(1)-C(7)	1.692(16)
Cu(1)-S(1)	2.240(9)	S(3)-C(8)	1.655(14)
Cu(1)-S(1')	2.314(8)	S(4)-C(9)	1.630(17)
Cu(1)-S(3')	2.319(6)	S(6)-C(88)	1.674(14)
Cu(1)-S(3)	2.321(7)	S(7)-C(94)	1.664(14)
Cu(2)-S(6')	2.143(5)	S(8)-C(45)	1.638(14)
Cu(2)-S(5)	2.1810(17)	S(1')-C(7')	1.654(15)
Cu(2)-S(7)	2.225(5)	S(3')-C(8')	1.696(13)
Cu(2)-S(6)	2.392(5)	S(4')-C(9')	1.686(15)
Cu(2)-S(7')	2.455(5)	S(7')-C(94')	1.679(14)
S(2)-C(14)	1.740(5)	S(6')-C(88')	1.656(15)
S(5)-C(65)	1.737(5)	S(9)-C(45')	1.620(14)

Table S6. Selected bond angles [°] for the complex [Cu^I(S-NHCH)(SS-NHC=S)] (**1**).

S(2)-Cu(1)-S(1)	133.1(2)	S(5)-Cu(2)-S(7')	118.80(12)
S(2)-Cu(1)-S(1')	133.6(2)	C(14)-S(2)-Cu(1)	104.54(17)
S(2)-Cu(1)-S(3')	127.91(16)	C(65)-S(5)-Cu(2)	99.5(2)
S(1')-Cu(1)-S(3')	95.9(2)	C(7)-S(1)-Cu(1)	94.4(6)
S(2)-Cu(1)-S(3)	127.26(17)	C(8)-S(3)-Cu(1)	92.0(5)
S(1)-Cu(1)-S(3)	97.5(3)	C(88)-S(6)-Cu(2)	94.0(5)
S(6')-Cu(2)-S(5)	143.34(15)	C(94)-S(7)-Cu(2)	96.5(5)
S(5)-Cu(2)-S(7)	132.38(13)	C(7')-S(1')-Cu(1)	94.7(5)
S(5)-Cu(2)-S(6)	131.44(13)	C(8')-S(3')-Cu(1)	94.0(5)
S(7)-Cu(2)-S(6)	95.22(17)	C(94')-S(7')-Cu(2)	90.3(5)
S(6')-Cu(2)-S(7')	96.87(17)	C(88')-S(6')-Cu(2)	97.9(5)

Computational Methods:

With the use of DFT, the complexes are optimized using hybrid functional B3LYP[S2-4] along with the dispersion correction term (D3(BJ))[S5-6], and the Ahlrichs triple-ζ-quality basis set def2-TZVPP[S7] using the Gaussian16[S8] package in the gaseous phase. The geometry optimization is favoured by minima on the potential energy surface followed by no negative

frequency, with the Dipp group replaced by the methyl group for calculation convenience. The NBO 6.0 program[S9] is used to perform the NBO[S10] calculations of the complexes, spin densities, mulliken charges, HOMO-LUMO energy gap and natural bond orbitals at B3LYP-D3(BJ)/Def2-TZVPP. To study the bonding behaviour of electrons in these complexes, we have adopted the energy decomposition analysis (EDA)[S11] coupled with natural orbital for chemical valence (NOCV)[S12-13] using the ADF 2020 program package[S14], which gives deep insight into the bond formation process between different fragments. It also gives the flexibility to study the interacting fragment in more than one possible charge and electron configuration. The previously optimized geometries at the B3LYP-D3(BJ)/Def2TZ2P level are used to carry out EDA-NOCV[S15-16] calculations at the same level of theory. ADF (Amsterdam Density Functional) program follows the Morokuma-type energy decomposition method, which involves the breakdown of overall energy into two components, ΔE_{prep} and ΔE_{int}, where E_{prep} gives the energy required to deform the fragments into acquired geometry and valence electronic configuration, while ΔE_{int} is the total interaction energy of those two fragments to form the complex again. ΔE_{int} is further split into four physical components in the ADF output file as,

$$\Delta E_{int} = \Delta E_{elstat} + \Delta E_{Pauli} + \Delta E_{orb} + \Delta E_{disp}$$

Table S7. The EDA-NOCV results at the UB3LYP-D3(BJ)/Def2-TZ2P level of theory of Cu-complex with SS-NHC=S$^{\cdot\,-}$ in doublet state and Cu(S-NHC-H)$^+$ in the singlet electronic state as interacting fragments of **1′**. Energies are in kcal/mol. [a]The values in the parentheses show the contribution to the total attractive interaction $\Delta E_{elec} + \Delta E_{orb} + \Delta E_{disp}$[a], and [b] value in the parentheses shows the contribution to the total orbital interaction.

Energy	Interaction	Cu-complex (**1′**)
ΔE_{int}		-140.2
ΔE_{Pauli}		118.4
ΔE_{disp}[a]		-9.7 (3.8%)
ΔE_{elstat}[a]		-181.3 (70.1%)
ΔE_{orb}[a]		-67.6 (26.1%)
$\Delta E_{orb(1)}$[b]	(SS-NHC=S$^{\cdot\,-}$) → Cu(I)(S-NHCH)$^+$ σ e$^-$ donation	-28.6 (42.3%)
$\Delta E_{orb(2)}$[b]	(SS-NHC=S)$^{\cdot\,-}$ → Cu(I)(S-NHCH)$^+$ π e$^-$ donation	-8.9 (13.2%)
$\Delta E_{orb(3)}$[b]	(SS-NHC=S)$^{\cdot\,-}$ → Cu(I)(S-NHCH)$^+$ σ e$^-$ donation	-4.2 (6.2%)
$\Delta E_{orb(4)}$[b]	(SS-NHC=S)$^{\cdot\,-}$ → Cu(I)(S-NHCH)$^+$ π e$^-$ donation	-2.4 (3.6%)
$\Delta E_{orb(rest)}$[b]		-23.5 (34.8%)
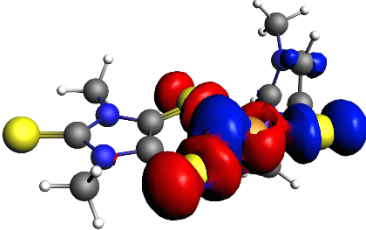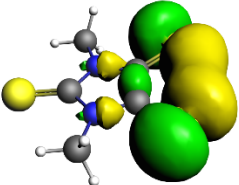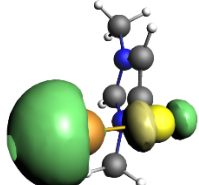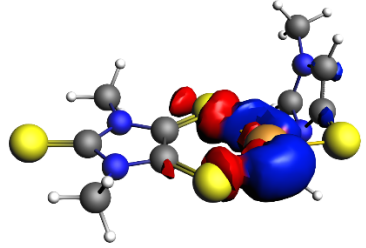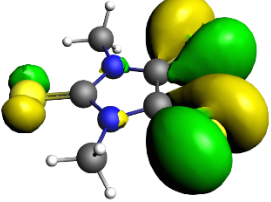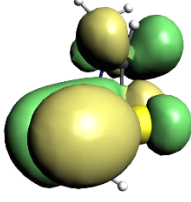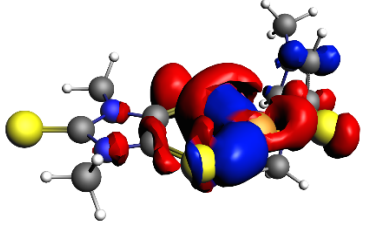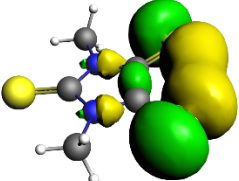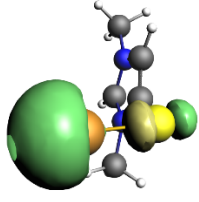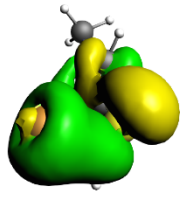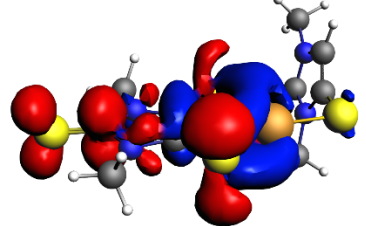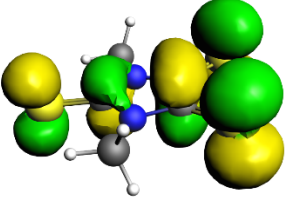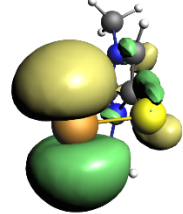
((SS-NHC=S)$^{\cdot-}$)Cu(I)(S-NHCH)	(SS-NHC=S)$^{\cdot-}$ (D)	Cu(I)(S-NHCH)$^+$ (S)
$\Delta\rho_{(1)}$ $\Delta E_{orb(1)} = -28.6$; $|v_1| = 0.52$	HOMO-1 ($\varepsilon = -2.24$ eV)	LUMO ($\varepsilon = -6.63$ eV)
$\Delta\rho_{(2)}$ $\Delta E_{orb(2)} = -8.9$; $|v_2| = 0.28$	HOMO ($\varepsilon = -1.76$ eV)	LUMO+2 ($\varepsilon = -4.16$ eV)
$\Delta\rho_{(3)}$ $\Delta E_{orb(3)} = -4.2$; $|v_3| = 0.14$	HOMO-1 ($\varepsilon = -2.24$ eV)	LUMO ($\varepsilon = -6.63$ eV) HOMO-1 ($\varepsilon = -10.39$ eV)
$\Delta\rho_{(4)}$ $\Delta E_{orb(4)} = -2.4$; $|v_4| = 0.11$	SOMO ($\varepsilon = +0.04$ eV)	LUMO+4 ($\varepsilon = -3.18$ eV)

Figure S6. The shape of the deformation densities $\Delta\rho_{(1)-(4)}$ that correspond to $\Delta E_{orb(1)-(4)}$, and the associated fragments orbitals of (SS-NHC=S)$^{\cdot-}$ in doublet state and Cu(I)(S-NHCH)$^+$ in the singlet electronic state of **1′** at the B3LYP-D3(BJ)/TZ2P level. The isosurface values are 0.001 au, 0.0001

and 0.0002 for $\Delta\rho_{(1-2)}$, $\Delta\rho_{(3)}$ and $\Delta\rho_{(4)}$ respectively. The eigenvalues $|v_n|$ give the size of the charge migration in e. The charge flow direction of the deformation densities is from red→blue.

EPR Measurements:
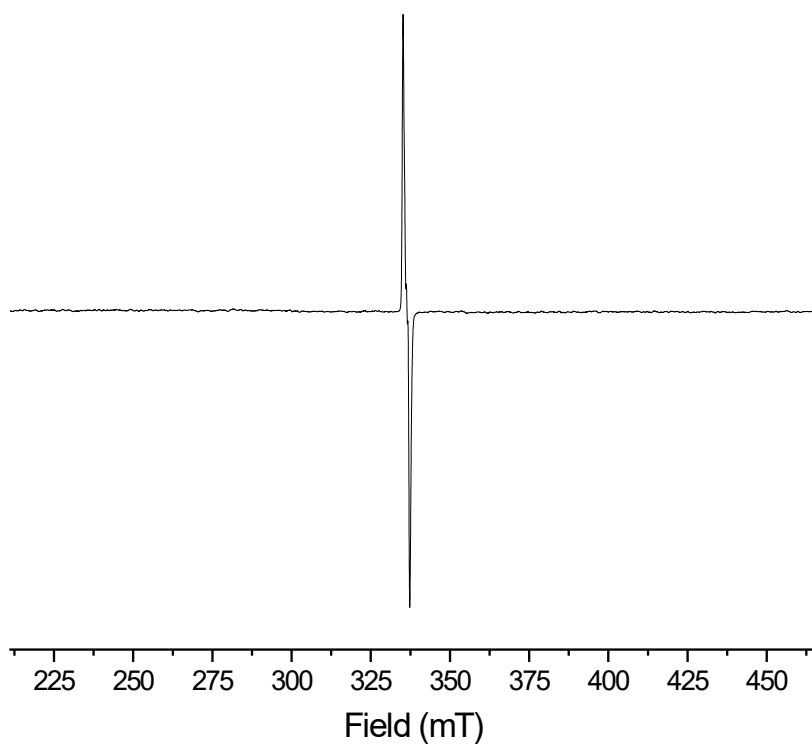

Figure S7. X-band EPR spectrum (black) of Cu(I)-radical complex (**1**) in in the range of 200-500 mT at 297 K in THF at higher concentration (3×10^{-4} M/L). The characteristic EPR bands due to Cu(II) ion is not observed.
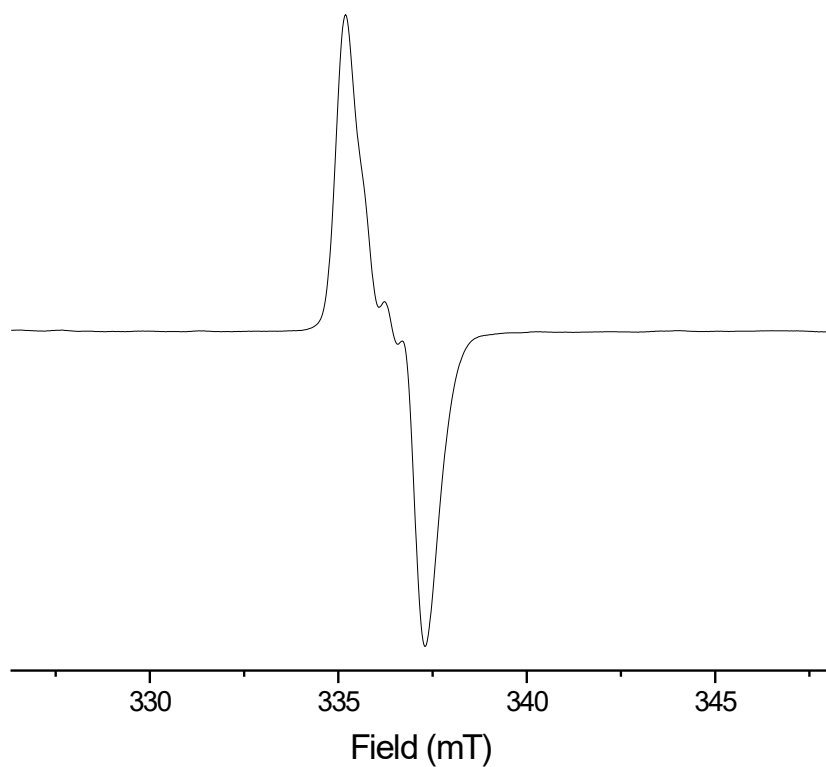
Figure S8. X-band EPR spectrum (black) of Cu(I)-radical complex (**1**) in the range of 320-500 mT at 297 K in THF solution, at higher concentration (3×10^{-4} M/L). The characteristic EPR bands due to Cu(II) ion is not observed (hump like EPR resonance < 335 mT).
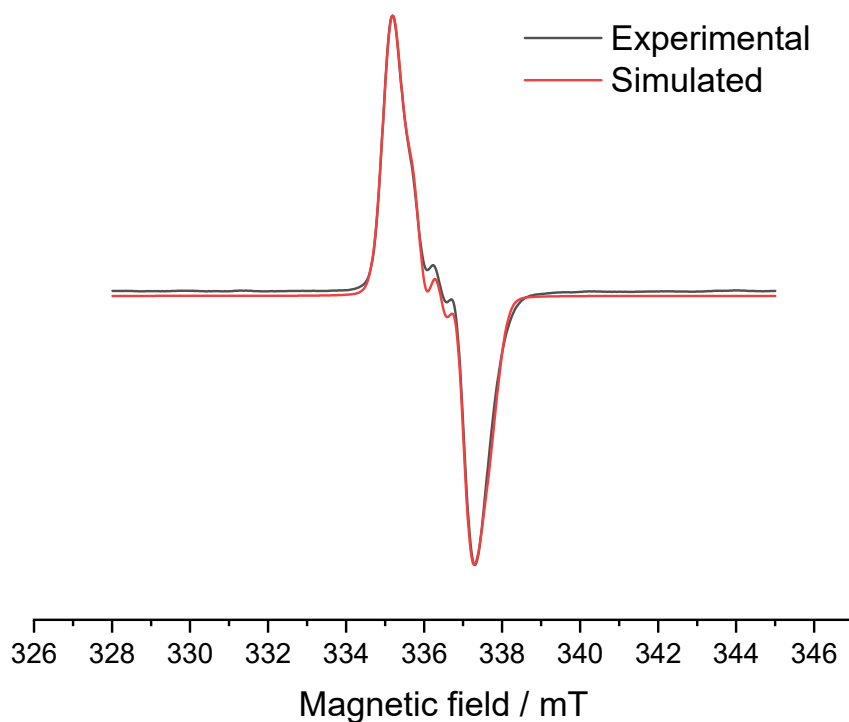
Figure S9. X-band EPR spectrum (black) of Cu(I)-radical complex (**1**) in the range of 320-500 mT at 297 K in THF at higher concentration (3×10^{-4} M/L). Red and black lines represent the simulated and the experimental spectra of Cu(I)-radical complex (**1**) using EasySpin program. [g_x = 2.00392, g_y = 2.00848, g_z = 2.00848, LWPP(Gaussian broadening) = 0.508581 mT, LWPP (Lorentzian broadening) = 0.0286045 mT, A(^{63,65}Cu)) = 14.5578 MHz, Experimental frequency = 9.452349 GHz].
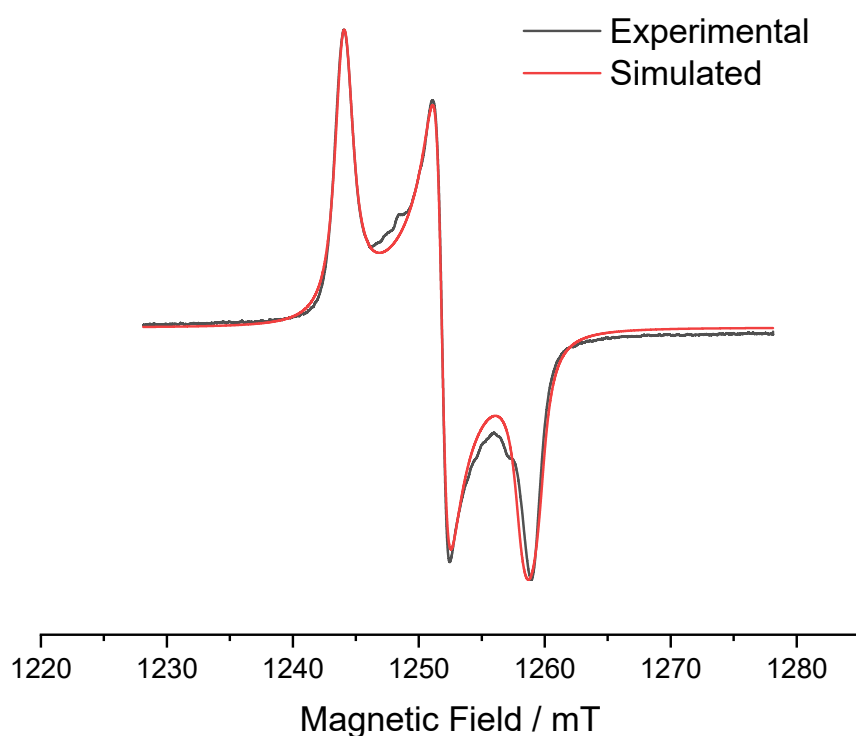
Figure S10. Q-band EPR spectrum (black) of Cu(I)-radical complex (**1**) in solid state. Red and black lines represent the simulated and the experimental spectra of Cu(I)-radical complex (**1**) using EasySpin program. [g_x = 2.02216, g_y = 2.00959, g_z = 1.99841, LWPP (Gaussian broadening) = 0.000586543 mT, LWPP (Lorentzian broadening) = 0.839682 mT; ^{63,65}Cu: A_x = 6.10525 MHz, A_y = 0.0560161 MHz, A_z = 13.0644 MHz, principal values of axial dipolar coupling tensor, dip_x = 7.60077 MHz, dip_y = 9.13918 MHz, dip_z = 24.3547 MHz, Q - band experimental frequency = 35.210000 GHz]. Average g = 2.010076.
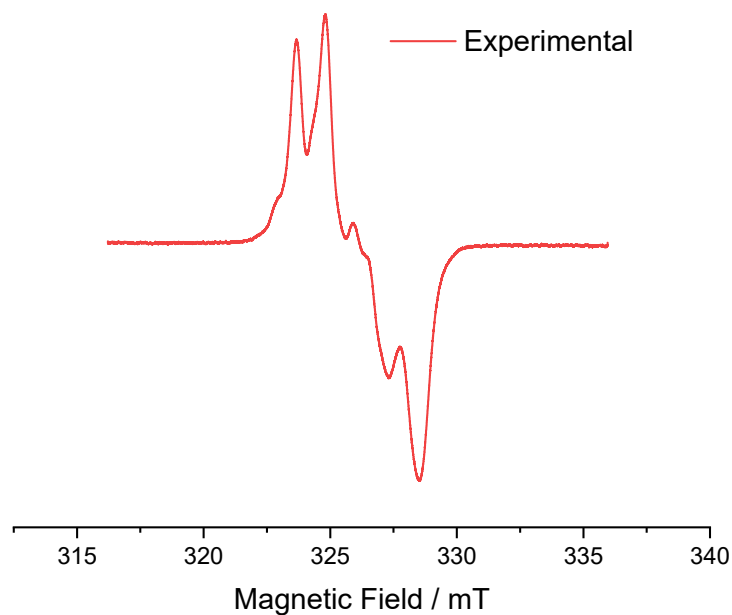
Figure S11. X-band EPR spectrum (red) of Cu(I)-radical complex (**1**) in frozen THF at 77 K. Experimental frequency = 9.171587 GHz.
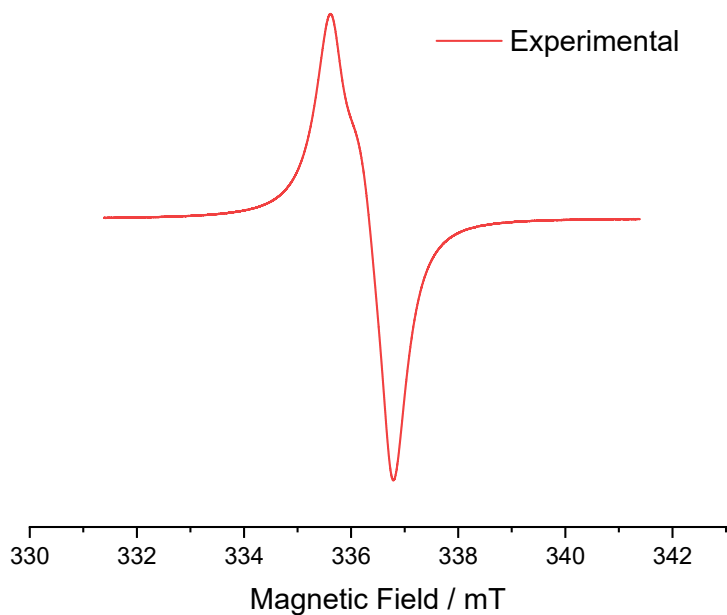
Figure S12. X-band EPR spectrum (red) of Cu(I)-radical complex (**1**) in solid state at 297 K. Experimental frequency = 9.452801 GHz.

XPS Plots of complex 1:

Figure S13. XPS plots for C-atoms in complex **1**.

Figure S14. XPS plots for N-atoms in complex **1**.

Figure S15. NBO charges in modelled **1′**.

Figure S16. TGA of complex **1** in open air over 90 min scanning the temperature from 30 °C to 930 °C.

References:

S1.   Y. Wang, H. P. Hickox, Y. Xie, P. Wei, S. A. Blair, M. K. Johnson, H. F. Schaefer III and G. H. Robinson, A Stable Anionic Dithiolene Radical. *J. Am. Chem. Soc*., 2017, **139**, 6859−6862.
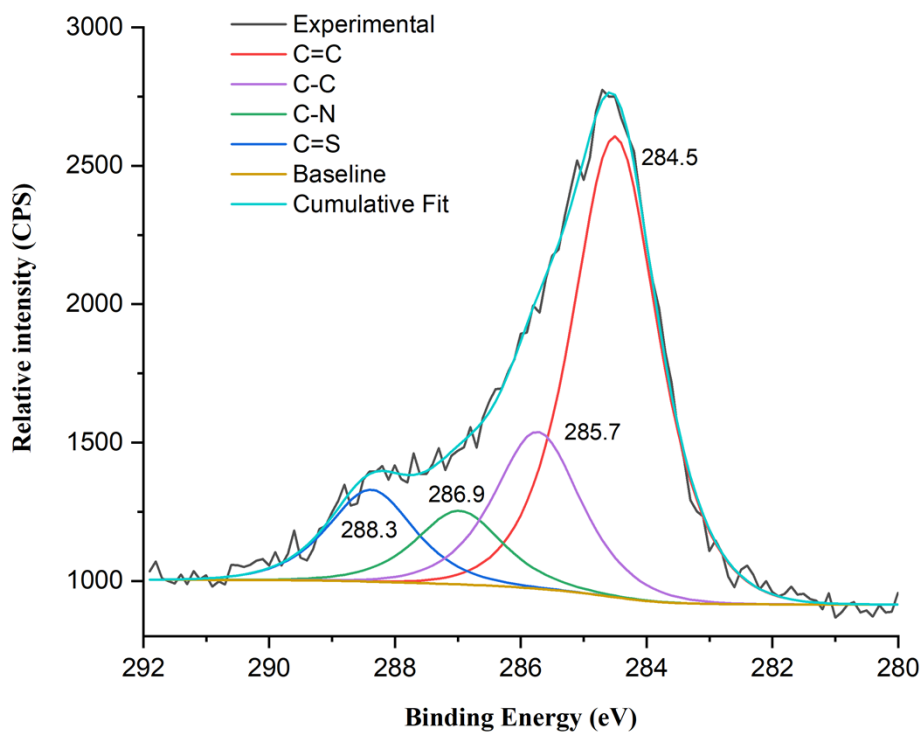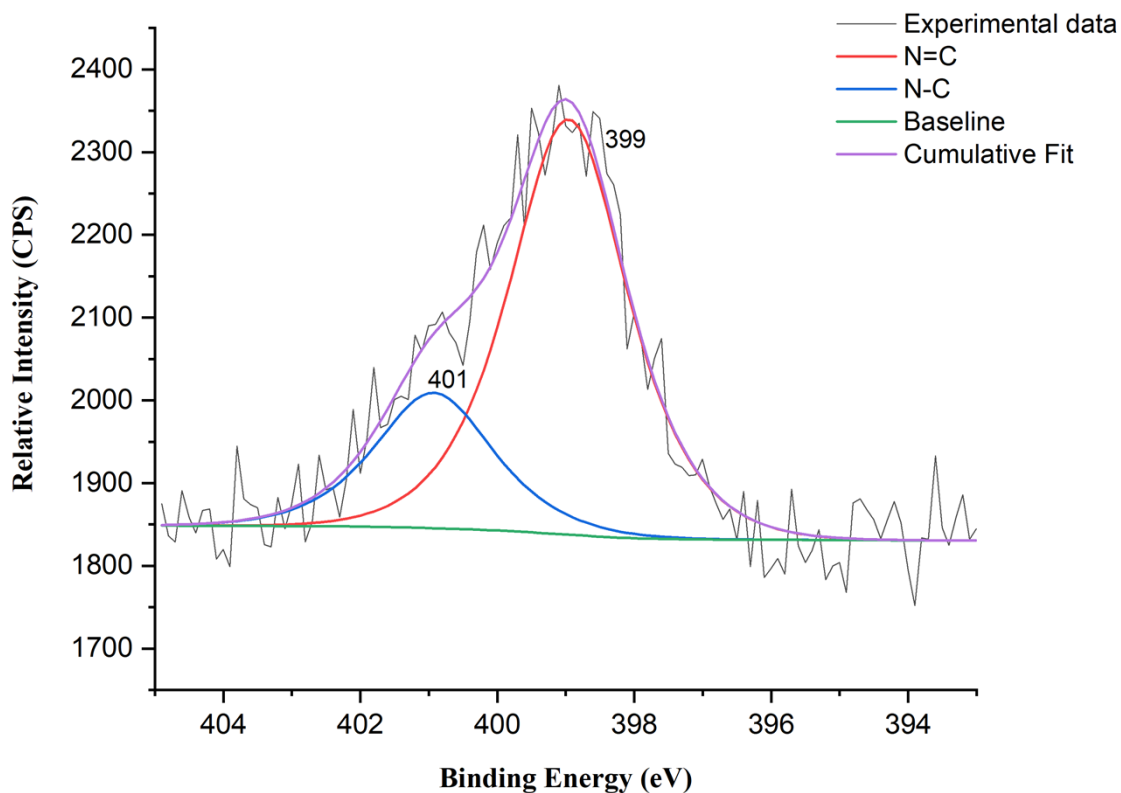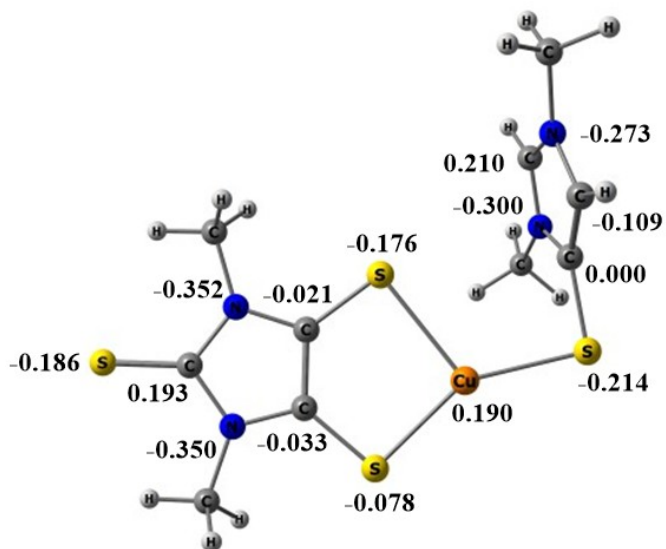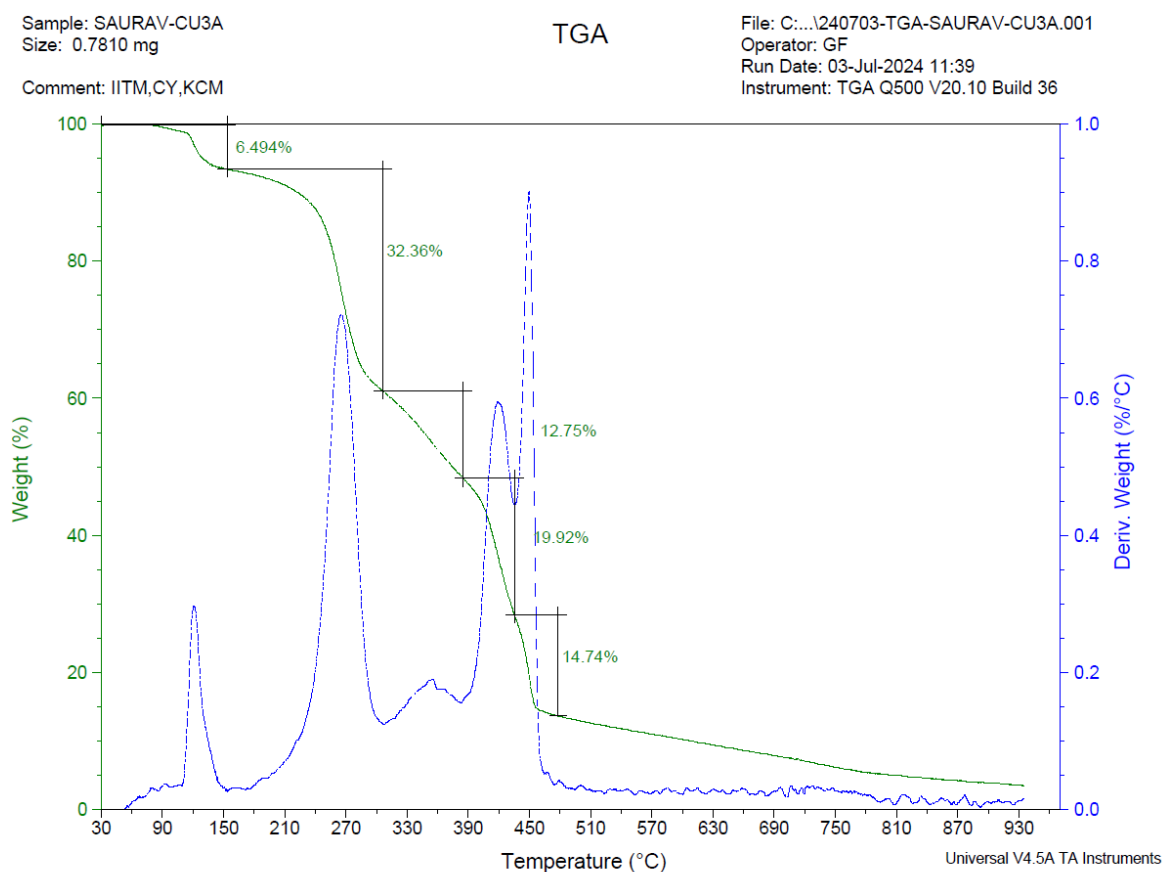
S2.   Becke, A. D. A new mixing of Hartree-Fock and local density-functional theories. *J. Chem. Phys.* **1993**, *98*, 1372-1377.

S3.   Stephens, P. J.; Devlin, F. J.; Chabalowski, C. F.; Frisch M. J. Ab Initio Calculation of Vibrational Absorption and Circular Dichroism Spectra using Density Functional Force Fields *J. Phys. Chem.* **1994**, 98, 11623-11627.

S4.   Lee, C.; Yang, W.; Parr, R. G. Development of the Colle-Salvetti correlation-energy formula into a functional of the electron density *Phys. Rev. B* **1988**, 37, 785-789.

S5.   Grimme, S.; Antony, J.; Ehrlich, S.; Krieg, H. A consistent and accurate ab initio parametrisation of density functional dispersion correction (DFT-D) for the 94 elements H-Pu *J. Chem. Phys*. **2010**, *132*, 154104-154124.

S6.   Grimme, S.; Ehrlich, S.; Goerigk, L. Effect of the damping function in dispersion corrected density functional theory. *J. Comput. Chem.* **2011**, *32*, 1456-1465.

S7.   Weigend, F.; Ahlrichs, R. Balanced basis sets of split valence, triple zeta valence and quadruple zeta valence quality for H to Rn: Design and assessment of accuracy. *Phys. Chem. Chem. Phys.* **2005**, *7*, 3297-3305.

S8.   Gaussian 16, Revision A.03, Frisch, M. J.; Trucks, G. W.; Schlegel, H. B.; Scuseria, G. E.; Robb, M. A.; Cheeseman, J. R.; Scalmani, G.; Barone, V.; Petersson, G. A.; Nakatsuji, H.; Li, X.; Caricato, M.; Marenich, A. V.; Bloino, J.; Janesko, B. G.; Gomperts, R.; Mennucci, B.; Hratchian, H. P.; Ortiz, J. V.; Izmaylov, A. F.; Sonnenberg, J. L.; Williams-Young, D.; Ding, F.; Lipparini, F.; Egidi, F.; Goings, J.; Peng, B.; Petrone, A.; Henderson, T.; Ranasinghe, D.; Zakrzewski, V. G.; Gao, J.; Rega, N.; Zheng, G.; Liang, W.; Hada, M.; Ehara, M.; Toyota, K.; Fukuda, R.; Hasegawa, J.; Ishida, M.; Nakajima, T.; Honda, Y.; Kitao, O.; Nakai, H.; Vreven, T.; Throssell, K.; Montgomery, J. A., Jr.; Peralta, J. E.; Ogliaro, F.; Bearpark, M. J.; Heyd, J. J.; Brothers, E. N.; Kudin, K. N.; Staroverov, V. N.; Keith, T. A.; Kobayashi, R.; Normand, J.; Raghavachari, K.; Rendell, A. P.; Burant, J. C.; Iyengar, S. S.; Tomasi, J.; Cossi, M.; Millam, J. M.; Klene, M.; Adamo, C.; Cammi, R.; Ochterski, J. W.; Martin, R. L.; Morokuma, K.; Farkas, O.; Foresman, J. B.; Fox, D. J. Gaussian, Inc., Wallingford CT, **2016.**

S9.   Glendening, E. D.; Landis, C. R.; Weinhold, F. NBO 6.0: Natural bond orbital analysis program *J. Comput. Chem.* **2013**, *34*, 1429-1437.

S10.   Reed, A. E.; Curtiss, L. A.; Weinhold, F. Intermolecular Interactions from a Natural Bond Orbital, Donor-Acceptor Viewpoint. *Chem. Rev.* **1988**, *88*, 899-926.

S11.   Ziegler, T., Rauk, A. On the calculation of bonding energies by the Hartree Fock Slater method. *Theor. Chim. Acta* **1977**, *46*, 1–10.

S12.   Mitoraj, M.; Michalak, A. Donor-Acceptor Properties of Ligands from the Natural Orbitals for Chemical Valence *Organometallics* **2007**, *26*, 6576 – 6580.

S13.   Mitoraj, M.; Michalak, A. Applications of natural orbitals for chemical valence in a description of bonding in conjugated molecules. *J. Mol. Model.* **2008**, *14*, 681-687.

S14.   *ADF2020, SCM, Theoretical Chemistry*; Vrije Universiteit: 782 Amsterdam, The Netherlands http://www.scm.com

S15.   Michalak, A.; Mitoraj, M.; Ziegler, T. Bond Orbitals from Chemical Valence Theory. *J. Phys. Chem. A* **2008**, *112*, 1933-1939.

S16.   Mitoraj, M. P.; Michalak, A.; Ziegler, T. A Combined Charge and Energy Decomposition Scheme for Bond Analysis. *J. Chem. Theory Comput.* **2009**, *5*, 962-975.

The Optimized Coordinate of Cu-complex at B3LYP-D3(BJ)/TZVPP

Cu-complex (**1′**) in doublet spin multiplicity

E = -3842.3759278 hf

Cu	-0.692292000	-1.563088000	-0.230100000
S	-2.891317000	-2.032938000	-0.219946000
S	1.457926000	-2.300254000	-0.182847000
S	-0.140120000	0.812471000	-0.142247000
C	-3.359553000	-0.383043000	-0.092550000
N	-4.000715000	1.733555000	-0.408333000
C	-3.619479000	1.629900000	0.863071000
C	-3.857464000	0.503245000	-1.019373000
N	-3.246005000	0.369118000	1.089794000

N	3.516256000	-0.510394000	-0.033514000
C	2.163299000	-0.767672000	-0.098819000
C	1.517095000	0.499501000	-0.079619000
S	5.242261000	1.597091000	0.115678000
C	3.765966000	0.843459000	0.025489000
N	2.521776000	1.439873000	-0.005274000
H	-4.076394000	0.354067000	-2.058862000
C	-4.443544000	2.953568000	-1.061770000
H	-3.743121000	3.222734000	-1.850050000
H	-5.433168000	2.805545000	-1.489315000
H	-4.485127000	3.755834000	-0.330392000
C	-2.697966000	-0.137437000	2.336574000
H	-3.143563000	-1.105382000	2.546795000
H	-1.621240000	-0.258752000	2.229804000
H	-2.920677000	0.569157000	3.131748000
C	4.536082000	-1.538517000	-0.030132000
H	4.389398000	-2.198612000	0.823438000
H	4.465236000	-2.129275000	-0.942170000
H	5.502925000	-1.049748000	0.030392000
C	2.294615000	2.867976000	0.032264000
H	1.752518000	3.177233000	-0.860203000
H	1.698126000	3.123614000	0.907106000
H	3.261692000	3.358398000	0.077856000
H	-3.603635000	2.431890000	1.577032000

Cu-complex (**1′**) in quartet spin multiplicity

E = -3842.2901424 hf

Cu	-0.547604000	-0.365175000	-0.920670000
S	-2.637070000	-0.510750000	-1.545716000
S	0.994529000	-1.874421000	-0.100394000
S	0.853376000	1.479867000	-0.961072000
C	-3.711725000	-0.137534000	-0.283812000
N	-5.645402000	0.197308000	0.799526000
C	-4.600583000	0.466003000	1.739737000

C	-5.088552000	-0.118626000	-0.408895000
N	-3.415272000	0.189157000	1.040376000
N	3.513411000	-0.963841000	0.473606000
C	2.239070000	-0.734188000	0.017054000
C	2.181405000	0.639872000	-0.335220000
S	5.853206000	0.373377000	0.886487000
C	4.272357000	0.190536000	0.431581000
N	3.424671000	1.159579000	-0.071138000
H	-5.673132000	-0.344014000	-1.282086000
C	-7.022585000	0.495614000	1.068244000
H	-7.187540000	1.575570000	1.169911000
H	-7.640550000	0.125901000	0.253036000
H	-7.336687000	0.012981000	1.995359000
C	-2.121579000	0.503988000	1.591651000
H	-1.387737000	-0.249343000	1.304795000
H	-1.760680000	1.484941000	1.270813000
H	-2.203184000	0.489468000	2.676384000
C	3.992133000	-2.251679000	0.934656000
H	3.386281000	-2.589097000	1.774090000
H	3.914391000	-2.981622000	0.130462000
H	5.027008000	-2.134093000	1.238754000
C	3.791930000	2.543175000	-0.296299000
H	3.661056000	2.790566000	-1.348527000
H	3.153559000	3.194317000	0.298844000
H	4.830265000	2.664816000	-0.005842000
H	-4.660285000	1.402118000	2.305789000